

# Simulation of severe thunder storm event: a case study over Pune, India

S. Fadnavis · Medha Deshpande · Sachin D. Ghude · P. Ernest Raj

Received: 21 August 2013 / Accepted: 10 January 2014 / Published online: 31 January 2014  
© Springer Science+Business Media Dordrecht 2014

**Abstract** Numerical simulation of a typical tropical thunder storm event at Pune (18.53°N, 73.85°E), India, has been performed using the three nested domain configuration of Weather Research and Forecasting-Advanced Research Weather Model (version 3.2). The model simulations have been compared with observations. Sensitivity to cumulus parameterization schemes, namely Betts–Miller (BM), Grell–Devenyi (GD), and Kain–Fritsch (KF), for simulation of vertical structure and time evolution of weather parameters has been evaluated using observations from automatic weather station and global positioning system radiosonde ascents. Comparison of spatial distribution of 24-h accumulated rain with Tropical Rainfall Measuring Mission data shows that BM scheme could simulate better rain than GD and KF schemes. The BM scheme could well simulate the development of storm and heavy rain as it could generate sufficiently humid and deep layer in the lower and middle atmosphere, along with co-existence of updrafts and downdrafts and frozen hydrometeors at the middle level and rain water near the surface.

**Keywords** WRF model · Cumulus parameterization schemes · Tropical thunder storm

## 1 Introduction

Weather prediction, especially in the tropical monsoon region, remains a significant challenge for numerical weather prediction systems. Prediction of thunderstorms is one of the most crucial tasks in weather prediction, due to smaller spatial and temporal scales and the inherent nonlinearity of their dynamics and physics. Regional models due to their dynamical and physical packages are able to disaggregate data at very high resolutions and predict weather and severe conditions. The inadequate treatment of subgrid convection is

---

S. Fadnavis (✉) · M. Deshpande · S. D. Ghude · P. Ernest Raj  
Indian Institute of Tropical Meteorology, Pashan Road, Pune 411008, India  
e-mail: suvarnafadnavis@gmail.com

widely believed to be a major impediment for improving the performance of numerical weather prediction (NWP) models in precipitation forecasting (Liu and Moncrieff 2007).

One of the essential steps in numerical weather simulation is to choose the best set of physics options for the region and time period under consideration. The sensitivity of cloud microphysics in predicting convective storms and precipitation has been addressed by many researchers (e.g., McCumber et al. 1991; Gilmore et al. 2004a, b; Reisner et al. 1998; Liu and Moncrieff 2007). Liu and Moncrieff (2007) evaluated the sensitivity of explicit simulations of coherent rainfall patterns to several bulk microphysical schemes using multiday cloud-system-resolving simulations at 3-km grid spacing. From comparison of four microphysical parameterization schemes, they reported that upper-level condensate and cloudiness, upper-level radiative cooling/heating and rainfall spectrum are the highly sensitive, whereas the domain-mean rainfall rate and areal coverage display moderate sensitivity. Few studies (Gallus 1999; Dudhia et al. 2003; Melissa and Mullen 2005) over Central United States have demonstrated that differences in cumulus parameterizations can have substantial impact on simulated storm convection and precipitation. Over the Indian region, sensitivity to physics parameterization and cumulus schemes for heavy rainfall events (Rama Rao et al. 2007; Litta et al. 2007; Litta and Mohankumar 2007; Vaidya and Kulkarni 2007; Kumar et al. 2008; Deb et al. 2008, 2010; Sukrit et al. 2010) and cyclones (Patra et al. 2000; Mandal et al. 2003, 2004; Mandal and Mohanty 2006; Trivedi et al. 2006; Rao and Prasad 2006, 2007; Srinivas et al. 2007; Ramalingeswara Rao et al. 2009; Deshpande et al. 2010; Mukhopadhyay et al. 2011; Osuri et al. 2012) has been reported adequately. The assessment of cumulus parameterization schemes in the short-range prediction of rainfall during the onset phase of the Indian Southwest Monsoon using MM5 Model has been reported by Dodla et al. (2012). Recently, numerical simulation studies related to thunderstorm evolution over the Indian region have been reported. The thunderstorm over Cochin (South India) is simulated using MM5 mesoscale model by Litta and Mohankumar (2007). They could simulate the rainfall pattern (GD scheme) and intensity with a time lag of 4 h. Chatterjee et al. (2008a, b) have shown the ability of MM5 in simulating severe/hail storm events over Gangetic Plain of West Bengal, India. Abhilash et al. (2008) have simulated the microphysical structure associated with tropical cloud clusters using MM5. Litta and Mohanty (2008) simulated features of a severe thunderstorm event observed over Northeast India (Kolkata) using WRF (NMM) model from field experiment data. They reported that high-resolution models have potential to provide unique and valuable information for severe thunderstorm forecasters. From RAMS model, Mukhopadhyay et al. (2005) analyzed the impact of assimilation of surface meteorological observations on thunderstorms and monsoon system. Rajeevan et al. (2010) have done cloud microphysics sensitivity experiments using WRF model to simulate severe thunderstorm event over Gadanki (Southeast India). They concluded that the thunderstorm simulation is very sensitive to microphysics schemes and there is large variability in the thunderstorm structure. This study emphasizes that along with the microphysics parameterization scheme, there is need to study the effect of cumulus parameterization schemes on the simulation of thunderstorm. Apart from the severe weather events, WRF model performance and sensitivity to model physics options are studied recently over Delhi, India, by Mohan and Bhati (2011). They performed sensitivity also to cumulus schemes. They considered surface and upper air meteorological parameters in summer and winter seasons. In general, the selection of surface layer, land surface model, and planetary boundary layer scheme was found to have more impact on output in comparison with microphysics and cumulus parameterization for both seasons. The study concluded that the model performance is satisfactory over the subtropical region of Delhi.

As can be seen from above discussion, detailed studies reporting thunderstorm simulations with cumulus parameterization over the Indian region are sparse. Studies on sensitivity of cumulus parameterization scheme to amounts of rain are very few. Hence, in the present study, an attempt has been made to understand the impact of three cumulus parameterization schemes, namely Betts–Miller (BM), Grell–Devenyi (GD) and Kain–Fritsch (KF), on the simulation of thunderstorm over Pune (18.53°N, 73.85°E), India. For this purpose, sensitivity experiments are carried out for the case of premonsoon thunder/hail storm day (June 1, 2010) over this station.

This paper includes details of data and model setup in Section 2. Section 3 illustrates results of simulation of thunderstorm event and comparison with observations. Performance of cumulus schemes is discussed by studying time evolution of stability parameters and vertical structure of relative humidity (RH), vertical velocity, and mixing ratio of hydrometeors in Sect. 4.

## 2 Model configuration and data

The Weather Research and Forecasting (WRF) model is developed for mesoscale modeling. The Advanced Research Weather WRF (WRF-ARW) model version 3.2 used in this study has dynamical core, which is fully compressible, Eulerian, and non-hydrostatic with a run-time hydrostatic option. It is conservative for scalar variables. The model uses terrain-following, hydrostatic pressure vertical coordinate with the top of the model being a constant pressure surface. The horizontal grid is the Arakawa-C grid. For time integration, model uses the third-order Runge–Kutta scheme, and the spatial discretization employs second- to sixth-order schemes. The model supports both idealized and real-data applications with various lateral boundary condition options (Dudhia 2010). The model physics package included the Rapid Radiative Transfer Model (RRTM) scheme for long-wave radiation, which is an accurate scheme using look-up tables for efficiency (Mlawer et al. 1997). It accounts for multiple bands, trace gases, and microphysics species. In Dudhia (1989) scheme for short-wave radiation, there is a simple downward integration, which allows clouds and clear-sky absorption and scattering. Surface layer scheme is based on Monin–Obukhov with Carlson–Boland viscous sublayer and standard similarity functions from look-up tables and five-layer thermal diffusion land surface scheme. We used Yonsei University Scheme (YUS) (Hong et al. 2006) for planetary boundary layer parameterization, which is a non-local K scheme with explicit entrainment layer and parabolic K profile in unstable mixed layer, WRF Single-Moment 6-class scheme (WSM-6) (Hong et al. 2004) for microphysics, which includes ice, snow, and graupel processes suitable for high-resolution simulations. Cumulus parameterization schemes are responsible for the subgrid-scale effects of convective and/or shallow clouds but are valid only for coarse grid sizes such as greater than 10 km. Among different cumulus parameterization schemes, Grell (Grell and Dévényi 2002), Betts–Miller (Janjic 1994, 2000), and Kain–Fritsch (Kain 2004) schemes are most widely used. Details about the KF scheme formulation and its various features are explained by Kain and Fritsch (1993), Gallus (1999), and Kain (2004). BM scheme is described by Betts (1986) and Betts and Miller (1986). This scheme has been used extensively in weather forecasts at the National Centers for Environmental Prediction (NCEP) and has been improved over the years (Betts and Miller 1986; Janjic 1994). The GD is a cloud ensemble scheme. The details of calculation of the ensemble mean are reported by Grell and Dévényi (2002).

Cumulus schemes are of primary importance for rainfall (Gallus 1999), in particular, in regions receiving predominantly convective rainfall, such as tropical areas (Dai 2006). Convective triggering is mostly initiated by lower-level dynamics, like moist convergence. The PBL schemes can affect temperature and moist profiles in the lower troposphere and interact with other schemes such as the convective parameterization and influence precipitation (Cr  tat et al. 2011 and references therein). PBL schemes are responsible for the turbulent mixing of all the levels which can trigger convection. Microphysics schemes play important role in controlling heat exchanges inside cloud and may have significant impact on radiative budget at surface and at the top of the atmosphere (Mukhopadhyay et al. 2011; Arakawa 2004).

Hence, it is important to choose appropriate combination of cumulus, PBL, and microphysics scheme to simulate a tropical thunderstorm. Simulations were performed with various combinations of PBL and MP schemes and cumulus parameterization. The WSM-6 for MP and Yonsei University Scheme for PBL show better performance; hence, they are fixed for all the experiments. To study the sensitivity to cumulus parameterization schemes, experiments were performed with three cumulus schemes, namely Grell–Devenyi (GD), Betts–Miller (BM), and Kain–Fritsch (KF). Table 1 shows the model configuration adopted for the present study. The model simulation was performed with two-way nesting at three nested domains D1, D2, and D3 with resolution of 50, 10, and 2 km, respectively (shown in Fig. 1). Initial and boundary conditions for three domains are obtained from NCEP FNL data set with  $1 \times 1$  horizontal resolution, which is interpolated to model grid resolution while preprocessing FNL data by model preprocessor (WPS). For D1 and D2, same cumulus parameterization schemes are used, which are excluded for D3. The model used 27 vertical levels with the top at 50 hPa.

National Centers for Environmental Prediction (NCEP) global final tropospheric analyses (FNL) data of resolution  $1^\circ$  are used as input for initial and boundary conditions to the model. The analyses are available on the surface and at 26 levels from 1,000 to 10 mb. In the present study, all experiments are conducted in the hind-cast mode with a time step of 1 h. The model boundary conditions are prepared from FNL analyses. For prediction purposes, FNL analyses will not be available; hence, NCEP GFS forecast should be used for preparing model boundary conditions. The lateral forcing is provided at every 6-h interval. The number of experiments was performed to study sensitivity of initial condition at 00UTC (5.30 am) of the same day, 12UTC (5.30 pm), and 00UTC (5.30 am) of the previous day. It is found that results obtained with the initial condition of 00UTC (5.30 am) of the same day show better simulation of a typical thunderstorm event. Litta and Mohanty (2008) also reported similar results. Hence, we use a cold start initialization at 00UTC (5.30 am) of the simulation day. Skamarock (2004) showed that small-scale structures are effectively spun over the initial 6–12 h. Hence, it provided us some confidence that our results for  $\geq 12$ -h simulation period were not unduly influenced by the simple cold start procedure. In the present study, model run is taken for pre-monsoon thunderstorm case of June 1, 2010, starting from 00UTC (5.30 am) model is integrated for 24 h. The GPS upper air sounding system used for the current observations is a Vaisala make DigiCORA Sounding System MW31, which consists of a PC connected to the Sounding Processing Subsystem SPS311 via a network adopter and contains the processor units for PTU (pressure, temperature, relative humidity) and wind finding and appropriate connections to directional UHF telemetry antenna used with the Sounding System to receive radiosonde signals in the 400-MHz meteorological band. It also includes Vaisala Radiosonde RS92, Ground Check Set GC25, and a GPS antenna. The details of the system are provided by He et al. (2009) and Turtiainen et al. (2010).

**Table 1** Overview of the WRF-ARW model configuration

Dynamics	Non-hydrostatic
Initial and lateral boundary condition data	NCEP FNL and RTG SST
Number of domains	Three (D1, D2 and D3)
Central point of domain D1	17°N, 73°E
Horizontal grid distance	D1—50 km, D2—10 km, D3—2 km
No. of horizontal grid points in X and Y directions	D1—135 × 115, D2—226 × 201, D3—201 × 176
Microphysics parameterization schemes (MPS)	WSM-6
Cumulus parameterization schemes (CPS)	Betts–Miller (BM), Grell–Devenyi (GD) and Kain–Fritsch (KF)
PBL parameterization scheme (PBL)	Yonsei University Scheme
Radiation parameterization scheme	RRTM for long wave and Dudhia for short wave
Soil model	Multilayer soil thermal diffusion model

To compare radiosonde data with model simulations, layer-averaged radiosonde values are centered at model level. (For example, 100-hPa model values are compared with 80–120-hPa layer-averaged radiosonde observation centered at 100 hPa.) On June 1, 2010, drift of radiosonde was 4–5 km radially, while on clear weather day on an average, drift was 2–3 km. Radiosonde movement was within the model inner domain D3.

Sea surface temperature values are obtained from NCEP's real-time, global, sea surface temperature analyses (RTG SST) available at a 0.5° resolution (Gemmill et al. 2007). Upper air data of temperature, relative humidity, wind speed, and direction are obtained from global positioning system (GPS) radiosonde (launched at Indian Institute of Tropical Meteorology campus, Pune, India (18.53°N, 73.85°E) on June 1, 2010, at 8UTC (1.30 pm)). The automatic weather station (AWS) data used for the validation of surface variables (temperature, relative humidity, 24-h accumulated rain, and mean sea-level pressure) have been obtained from the Web site <http://www.wunderground.com> for Pune station, and these data are available at 3-h interval. This Web site collects weather conditions directly from weather stations located in various countries, which are owned by government agencies and international airports.

The Tropical Rainfall Measuring Mission (TRMM) satellite provides unique measurements of horizontal and vertical profiles of precipitation. The TRMM carries precipitation radar (PR) and a microwave imager (TMI) that measures the outgoing microwave radiation at different frequencies. Details of TRMM measurements are documented at ([http://disc.sci.gsfc.nasa.gov/precipitation/documentation/guide/TRMM\\_dataset.gd.shtml](http://disc.sci.gsfc.nasa.gov/precipitation/documentation/guide/TRMM_dataset.gd.shtml)).

The TRMM Sun synchronous orbit is circular and is at an altitude of 350 km with an inclination of 35° to the equator. The spacecraft takes about 91 min to complete one orbit around the Earth. The PR has a data swath of 215 km and TMI 780 km. Together the PR and TMI data provide a unique measure of synoptic-scale rainfall. The 3B42 algorithm provides daily precipitation and root mean square (RMS) error estimates at 0.25° × 0.25° latitude/longitude grids over 50°N–50°S for version 6 (V6). In this study, the 3B42 version 6 product is used (Huffman et al. 2007). The TRMM 3-hourly data are aggregated for a day for the validation. On June 1, 2010, there was one pass of TRMM over Pune.

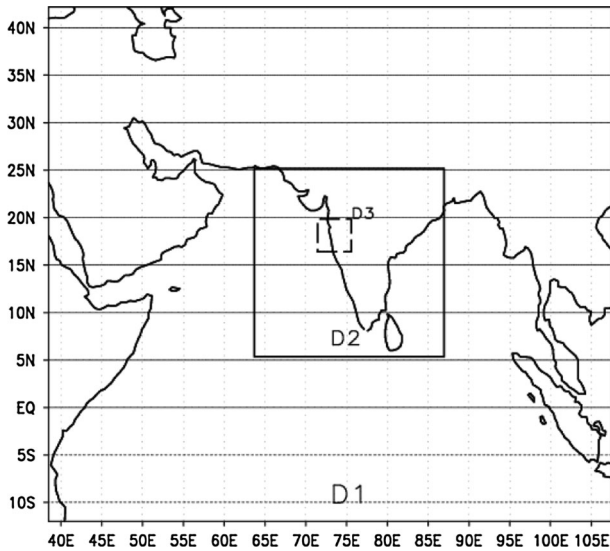


**Fig. 1** Model domain configuration used for WRF simulations

### 3 Results

#### 3.1 Simulation of thunderstorm on June 1, 2010

The WRF model simulations were performed for a heavy rain event/typical thunderstorm day ‘June 1, 2010’ (premonsoon severe thunderstorm). Model-simulated rainfall is compared with observed TRMM satellite data. Spatial distribution of 24-h accumulated rain in the domain 3 as observed by TRMM is plotted in Fig. 2. Model-simulated accumulated rain (for 24 h) in the same domain is shown in Fig. 3a–c for GD, BM, and KF schemes. The spatial distribution of difference between simulated and observed accumulated rain for GD, BM, and KF is plotted in Fig. 3d–f. It is quite evident that TRMM data show patch of rain aligned in southeast to northwest direction. Heavy rain (80–100 mm) is observed in region 18.6°N–19.8°N, 73.5°E–74.5°E. Similar to TRMM observations, model-simulated rain obtained from all the three schemes also shows patch of rain aligned in southeast to northwest directions. But model-simulated rain patch is shifted slightly westward when compared to TRMM observations. Model-simulated 24-h accumulated maximum rain (~80–100 mm) (although shifted spatially) quantitatively agrees with TRMM observations. However, TRMM data show that the maximum rain is concentrated between 8.6°N–19.8°N and 73.5°E–74.5°E while maximum rain obtained from cumulus schemes is distributed along the patch. Betts–Miller scheme shows rain over the Arabian Sea, which is observed neither in TRMM data nor in GD and KF simulations. Difference between simulated rain and TRMM observed rain (as can be seen from Fig. 3d–f) shows both positive and negative biases. This may be due to spatial shift in the simulated rainfall pattern. In general, positive bias is less for the case with KF cumulus scheme.

At 0800UTC (1.30 pm) of June 1, 2010, there was a special launch of global positioning system (GPS) radiosonde from IITM Pune (18.53°N, 73.85°E). The vertical profiles of temperature, relative humidity (RH), and wind speed and direction obtained for the three schemes were extracted at 8UTC (1.30 pm) at the grid centered at Pune (18.53°N, 73.85°E).

These profiles are compared with observations from radiosonde as shown in Fig. 4a–d, respectively. Figure 4a shows comparison of model-simulated temperature (BM, GD, and KF schemes) with temperature measurement of GPS radiosonde. Profiles of temperature obtained from all the three schemes indicate excellent agreement with observations throughout the troposphere. Both model simulations and observations show temperature  $\sim 310$  K near the surface. It then decreases with increase in height and reaches  $\sim 190$  K near the tropopause.

Vertical variation in relative humidity (RH) (%) at Pune at 0800UTC (1.30 pm) obtained from model simulations and GPS radiosonde observation is shown in Fig. 4b. Profiles of RH for BM, GD, KF schemes agree well with each other, indicating little sensitivity to cumulus parameterization. Very small almost negligible difference ( $\sim 3$  %) is observed near 100-mb pressure levels. Vertical profile of RH as observed by GPS sonde shows structure similar to profiles obtained from model simulations. Profiles of all the three schemes agree well with GPS radiosonde profile from surface to 750-mb pressure levels. Both model simulations and observations show peak near 700–750-mb pressure levels. Model-simulated RH peaks ( $\sim 95$  %) near 700 mb, while observed humidity peaks ( $\sim 80$  %) near 750-mb pressure level. At the altitudes above these pressure levels (700–750 mb), RH profiles decrease with increase in height. Model-simulated profiles attain minimum RH (10–12 %) near 150 mb, while GPS radiosonde profile shows minimum RH (1 %) near 400-mb pressure level. It is very interesting to note that RH  $\sim 100$  % is observed near 650 mb, which is due to the presence of the convective cloud. Similarly, variations are observed between 400–350 and 550–600-mb pressure levels, which may also due to the presence of cloud at these levels. These variations are not observed in the model-simulated profiles, which may be due to the fact that vertical resolution of observed data is very high when compared to model vertical resolution.

Vertical variation of wind speed as can be seen in Fig. 4c, d obtained from model simulation (BM, GD, KF) agrees well with the observation throughout the troposphere with some differences at the altitude above 500 mb. At the pressure level between 500 and 200 mb, model simulates higher wind speed than observation. BM shows higher deviation when compared to other schemes. While between 100- and 200-mb pressure level, model

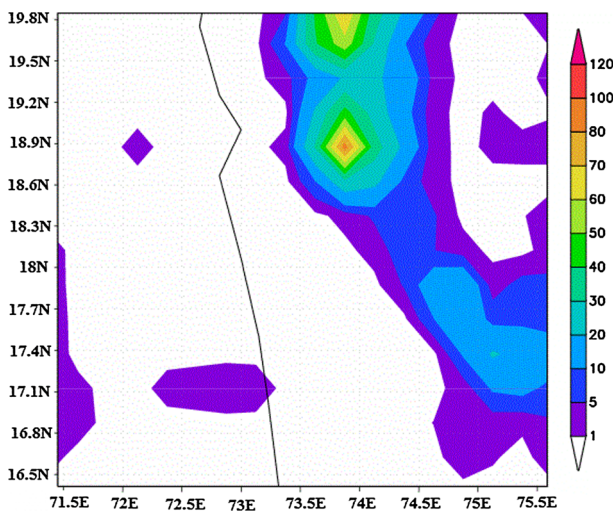


**Fig. 2** Spatial distribution of 24-h accumulated rain (mm) as obtained from TRMM on June 1, 2010

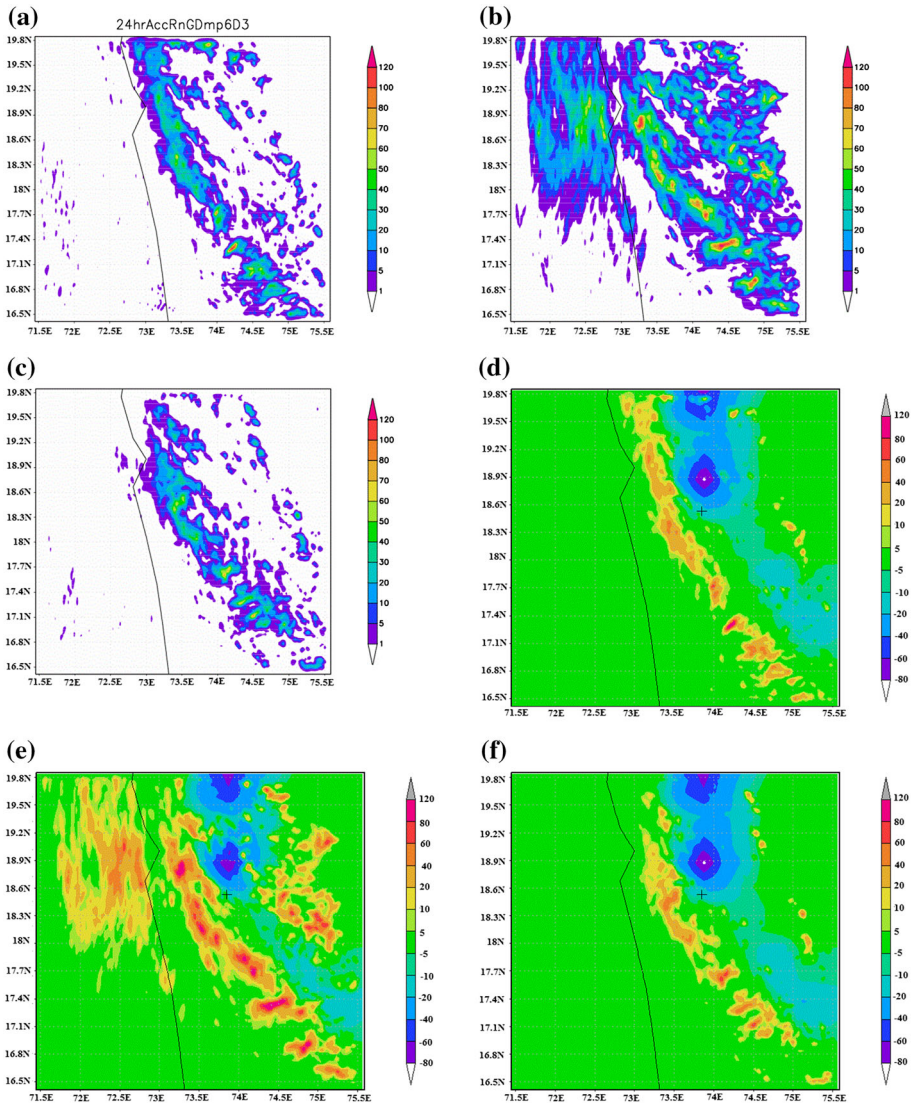


**Fig. 3** Spatial distribution of 24-h accumulated rainfall (mm) as obtained from model simulations for a GD, b BM and c KF and d TRMM-GD, e TRMM-BM, and f TRMM-KF on June 1, 2010

underestimated wind speed, but GD shows maximum deviation. Comparison of wind direction simulated by WRF model shows good agreement with observations from surface to 200-mb pressure levels. At the altitudes, above 200-mb level minor differences appear.

The storm initiation and development were examined by the analysis of temporal variation in surface pressure, temperature, relative humidity, and accumulated rainfall. Surface pressure and temperature are useful parameters in determining the likelihood of occurrence of a thunderstorm. The model-simulated time evolution of the meteorological parameters is compared with the available AWS data of Pune station. Figure 5a shows time evolution of



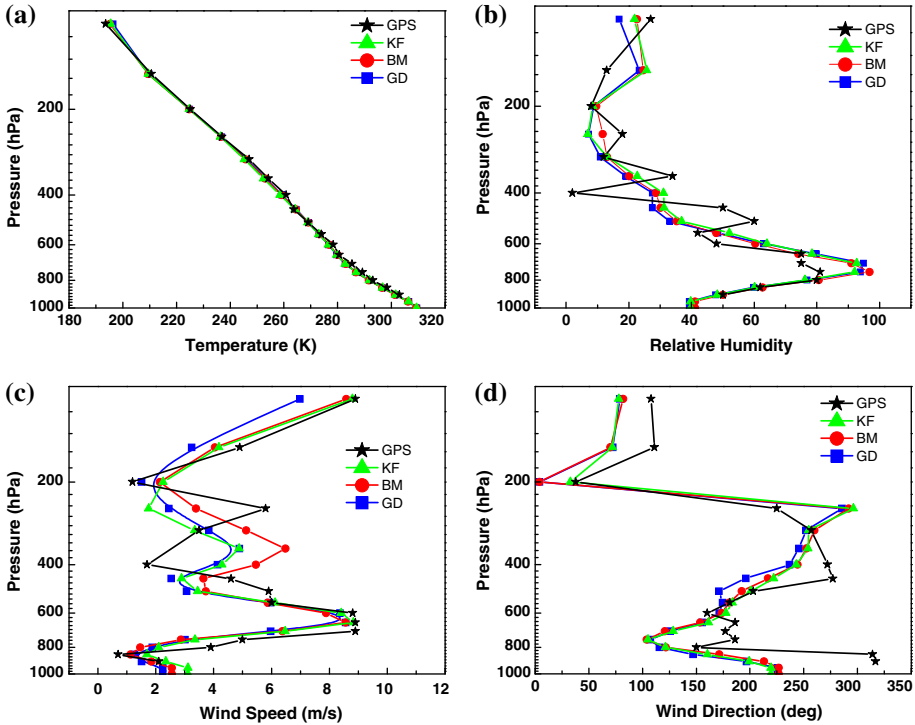


**Fig. 4** Verticals distribution of **a** temperature (K), **b** relative humidity (RH) (%), **c** wind speed (m/s) and **d** wind direction (*degrees*); simulated by WRF model KF (green color profile), GD (blue color profile), BM (red color profile), and AWS observation (black color profile) at 0800UTC (1.30 pm) of June 1, 2010

surface temperature as obtained from model simulations (all the three cumulus schemes) and AWS data. As evident from Fig. 5, model-simulated time evolution of temperature shows good agreement with observed (AWS) data from 0UTC (5.30 am) to 9UTC (2.30 pm). Model-simulated and observed temperature evolution shows differences from 9UTC (2.30 pm) onwards as thunderstorm event occurred during 9–12UTC (2.30–5.30 pm). Observed temperature starts decreasing from 9UTC (2.30 pm) and attains minimum at 12UTC (5.30 pm). All the three schemes show decrease in temperature from 8UTC (1.30 pm) but overestimate temperature after 9UTC (2.30 pm). The observed minimum temperature at 12UTC (5.30 pm) may be due to precipitation (see Fig. 5c). Sudden drop in surface temperature is also simulated by all the three schemes. Figure 5c shows time variation in precipitation as obtained from model simulations and AWS-observed precipitation. The model underestimates the precipitation at grid point containing Pune; hence, the temperature drop is also underestimated. Among the three schemes considered here, BM shows highest temperature drop and highest accumulated rain (Fig. 5a, c).

Relative humidity at the surface level has also been taken into account, as it is an essential factor for intense convection. Comparison of time evolution of RH as obtained from model simulations and AWS observations is shown in Fig. 5b. RH ~ 75 % is observed at 0UTC (5.30 am), and it then decreases with time and attains minimum at 9UTC (2.30 pm). Model could reproduce similar variations, but RH is overestimated. It is evident that model-

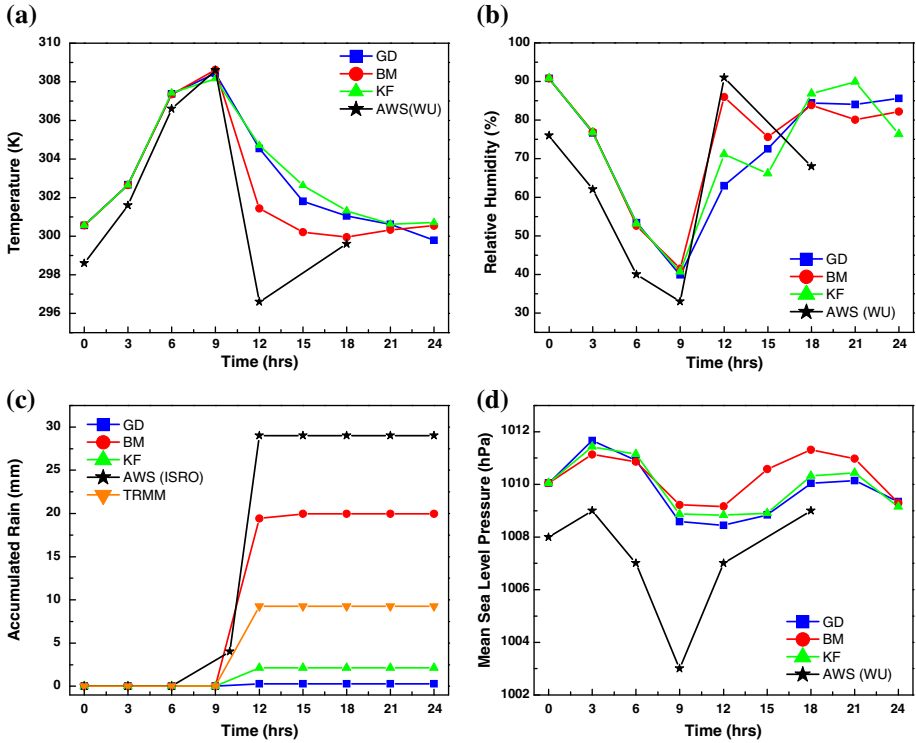


**Fig. 5** Time series of surface **a** temperature (K), **b** relative humidity (RH) (%), **c** accumulated rain (mm) and **d** sea-level pressure (hPa); simulated by WRF model KF (green color profile), GD (blue color profile), BM (red color profile) and AWS observation (black color profile) and TRMM precipitation (mm) for the case of June 1, 2010, thunderstorm

simulated RH attains minimum 1 h before the observation. (It should be noted that model-simulated temperature attains peak 1 h before the observations.) This may be due to sampling interval of AWS data (3 h). The model simulations show agreement with observation from 0UTC (5.30 am) to 9UTC (2.30 pm) after which observed RH and model-simulated RH for different schemes differ. BM scheme simulates peak in RH (83 %) at 12UTC (5.30 pm), but it underestimates when compared to observed (90 %).

Figure 5c shows time series of accumulated precipitation at Pune from 00UTC (5.30 am) on 1 June to 00UTC (5.30 am) 2 June as simulated by the model with three cumulus parameterization schemes. These results are then compared with AWS observation at Pune and TRMM data extracted over Pune. AWS data show precipitation started at 07UTC (12.30 pm), while TRMM and model simulations (all three schemes) indicate that precipitation started at 09UTC (2.30 pm). AWS data show heavy rain (~25 mm) between 10UTC (3.30 pm) and 11UTC (4.30 pm). However, TRMM data show 9-mm rain in 3 h (09–12UTC (2.30–5.30 pm)). The differences in precipitation as obtained from TRMM and AWS may be due to the fact that AWS observations are at single station (Pune), while precipitation obtained from TRMM data is averaged over a grid containing Pune. Model-simulated rain with BM scheme also shows sharp increase in rain ~18 mm in 1 h (09–10UTC (2.30–3.30 pm)). Then, simulated rain increases to 20 mm. Model simulation

with GD gives no rain throughout the integration period, while KF gives 2 mm rain in 1 h (09–10UTC (2.30–3.30 pm)). Simulated rain with BM is comparable with AWS and TRMM data. But KF and GD both failed to simulate heavy rain. Rain simulated by BM is less (by 9 mm) than AWS data but more than TRMM data (by 11 mm). Resolution of TRMM data is coarse compared with model resolution. Therefore, it may underestimate the rain. Moreover, model-simulated heavy rain has been shifted toward west. In Fig. 3d–f, ‘+’ sign indicates point location of Pune station at which model and TRMM data are extracted. Negative bias at this location indicates that rain is underestimated by the model.

Mean sea-level pressure simulated by WRF model is compared with observed AWS data (see Fig. 5d). Model-simulated diurnal variation in pressure shows bimodal distribution as observed by AWS data. However, it overestimates the pressure throughout the model integration period. There is sudden rise in pressure between 9UTC (2.30 pm) and 12UTC (5.30 pm) during the occurrence of the storm as observed from AWS plot, which is a characteristic feature of a thunderstorm (Brunk 1949; Litta and Mohanty 2008). The rise in pressure is captured by BM, GD, and KF schemes, but the occurrence is delayed by almost 3 h compared to that observed. Model-simulated mean sea-level pressure agrees well with each other before the occurrence of storm (10UTC (3.30 pm)). After the occurrence of storm, BM scheme shows higher pressure when compared to GD and KF. None of the scheme could simulate the minimum mean sea-level pressure of 1,003 mb at 9UTC (2.30 pm). Plot of mean sea-level pressure obtained from simulation with GD scheme shows minimum pressure of 1,007.5 hPa at 14UTC (7.30 pm).

Weather Research and Forecasting (WRF) model simulation (BM, KF, GD) of temperature, RH, rain, and sea-level pressure show good agreement with observations before the occurrence of storm (10UTC (3.30 pm)). After the occurrence of storm, only model simulations with BM scheme show better agreement with observed parameters (as can be seen from Fig. 5a–d).

#### 4 Discussions

The present analysis shows that 24-h accumulated precipitation on June 1, 2010, simulated by BM parameterization scheme is quantitatively closer in agreement with surface observations (AWS) than those with KF and GD schemes (Fig. 5c). Hence, in order to further understand the relationship, model-simulated stability indices, namely convective available potential energy (CAPE) and convective inhibition (CIN), for the three cumulus schemes are examined. CAPE is defined as vertically integrated all positive buoyancy values between 100 m and level of neutral buoyancy. CIN can be thought of as negative CAPE. Details of calculation of CAPE and CIN from radiosonde observations are explained by Molinari et al. (2012) and Romps and Kuang (2010). The time evolution of CAPE and CIN simulated using GD, BM, and KF at Pune on the thunderstorm day is depicted in Fig. 6a, b. CAPE and CIN values as obtained from radiosonde observations at 8UTC (1.30 pm) are 1,098 and 0 J/kg, respectively. At this time, model-simulated (by three schemes) CAPE is  $\sim 600$  J/kg and CIN is 0 J/kg. As model-simulated CAPE is less than observed values, this may be the reason that model has underestimated precipitations. Model simulations show sudden increase in CAPE at 09UTC (2.30 pm) (1–2 h before the occurrence of the storm) by all three cumulus schemes. CAPE simulated using KF is 1,400 J/kg, GD is 1,000 J/kg, and BM is 700 J/kg. During the same period, time evolution of CIN exhibits values  $\sim 250$  J/kg by GD,  $\sim 175$  J/kg by KF, and  $\sim 120$  J/kg by BM. Although CAPE simulated by KF and GD is higher than BM, their CIN values are also higher which might have inhibited the

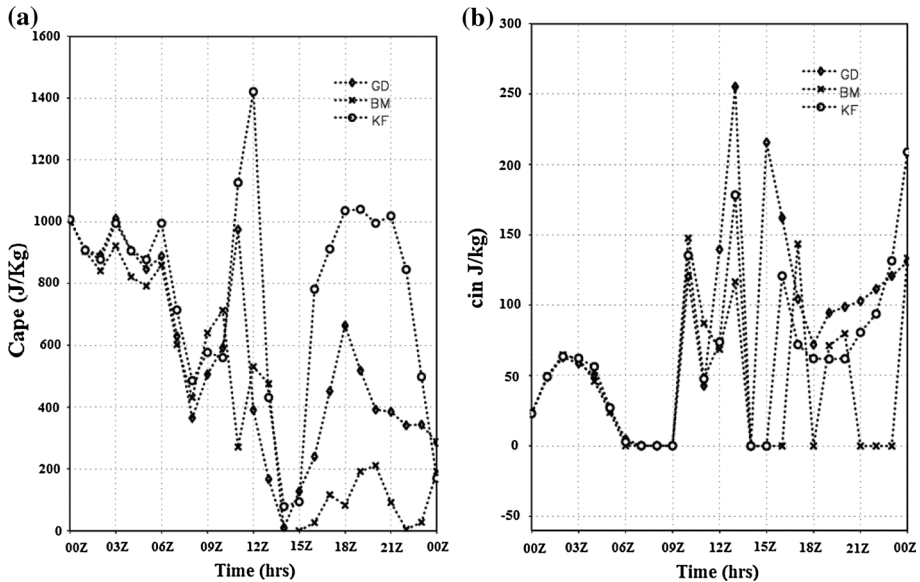


**Fig. 6** Time evolution of **a** CAPE (J/kg) and **b** CIN (J/kg) as simulated by model with GD (symbol of diamond), BM (symbol of multiplication), and KF (symbol of circle) on June 1, 2010

development of the storm. However, CAPE simulated by BM is less, still it could simulate the storm better than GD and KF as CIN simulated by BM is less.

Time–height cross section of RH (%), vertical velocity ( $w$ , m/s), and mixing ratio of hydrometeors (gm/kg) at a grid point containing Pune are plotted in Fig. 7a–i for all the three schemes. Storm development requires a sufficiently humid and deep layer in the lower and middle atmosphere (Johns and Doswell 1992; Litta and Mohankumar 2007). Figure 7a–c show time–height cross section of RH obtained from BM, GD, and KF simulations. It is evident that BM could simulate RH >90 % at mid-level (800–500 mb) during the period of thunderstorm (09–15UTC (2.30–8.30 pm)). It shows the presence of considerable amount of moisture, which remains high from the time of genesis of the thunderstorm to the time of precipitation. However, KF and GD could simulate RH <80 % at mid-levels. This may be one of the reasons for underestimation of precipitation simulated by KF and GD. Figure 7d–f shows time–height cross sections of model-simulated vertical velocity with different cumulus parameterization schemes. If a strong updraft and downdraft coexist side by side without mutual interference, a severe thunderstorm is likely to develop (Asnani 2005; Litta and Mohanty 2008). As can be seen from Fig. 7e, such coexistence of strong updraft and down drafts is well simulated by BM. GD also simulates the coexistence of downdraft–updraft but the updrafts are weak. The KF scheme showed much disorganized updraft/downdraft cores. Usually during the different phases of the thunderstorm, downdraft spreads in the lower parts of the storm after the initiation of rainfall (Litta and Mohankumar 2007). Plot of vertical velocity from BM (Fig. 7e) indicates strong patch of downdraft from surface to 100 mb level during 10–12UTC (3.30–5.30 pm) (after the onset of rainfall). This structure of downdraft is not observed in the case of GD and KF simulations, and these two schemes could not simulate the heavy rain. The updraft and downdraft motions depend on the heating associated with freezing

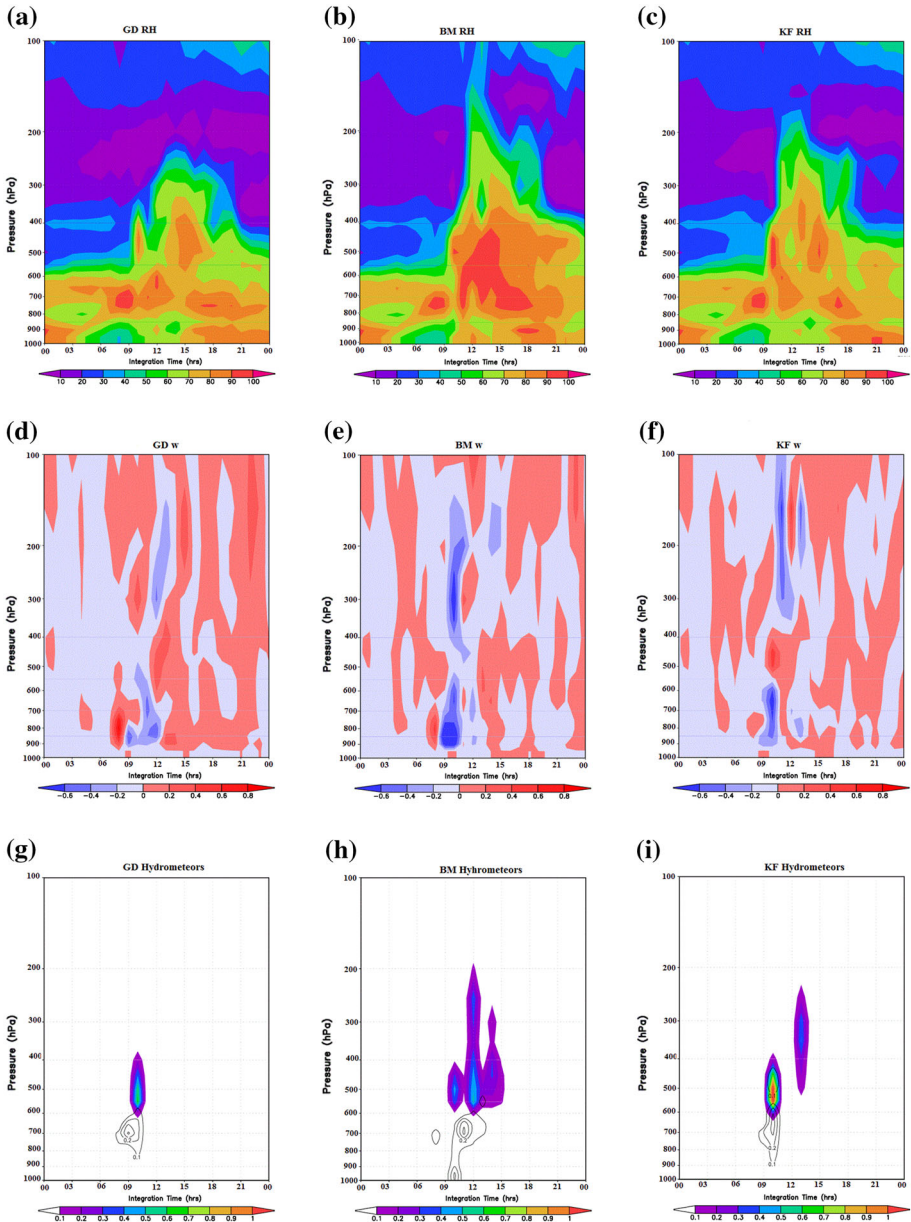


**Fig. 7** Time–height cross section of **a–c** relative humidity (%), **d–f** vertical velocity (m/s) and **g–i** mixing ratios of (frozen with shaded and liquid with contour) hydrometeors (gm/kg) at a grid point containing Pune as simulated by GB, BM, and KF on June 1, 2010

and cooling associated with melting. Also, there may be contribution from evaporation and condensation depending on the temperature. It is evident that water substance can take a variety of forms in a cloud. The various forms of water and ice coexist and interact within the cloud ensemble. The overall properties of the cloud ensemble are of primary interest in

cloud dynamics. The evolution of a cloud can be characterized in terms of fields of mixing ratios of all water substances. Hence, total hydrometeor content inside a cloud can be divided into cloud liquid water, rain water, cloud ice, snow, and graupel. The total water substance in a parcel of air is given by the sum of the water contained in each of the categories. The vertical distribution of the particle density of these species is important. Time–height variation in frozen (shaded) and liquid (contour) hydrometeors obtained from GD, BM, and KF is plotted in Fig. 7g–i. Here, the frozen hydrometeors indicate the mixing ratios of ice, snow, and graupel (gm/kg), whereas liquid hydrometeors indicate the mixing ratios of cloud and rain water in (gm/kg). The plot indicates that the cumulus parameterization schemes used in domain 1 and domain 2 have impact on the distribution of hydrometeors in domain 3 where no cumulus parameterization scheme is used, although the microphysics parameterization scheme is same (WSM-6) for all three domains and in all three experiments. GD shows single-cell structure, KF shows two cell structures, whereas BM shows three-cell structure of frozen hydrometeors between 09UTC (2.30 pm) and 15UTC (8.30 pm). The three-cell structure of hydrometeor shown by BM scheme indicates that hydrometeor distributed vertically up to 200 mb for longer time (09–15UTC (2.30–8.30 pm)). The liquid hydrometeors mixing ratio is almost same (0.3 gm/kg) at about 700-mb level for all three cumulus schemes, but only BM shows higher mixing ratio (3 gm/kg) near the surface between 10UTC (3.30 pm) and 11UTC (4.30 pm), which is due to rain water. This may be the reason for heavy precipitation ( $\sim 18$  mm) simulated by BM between 10UTC (3.30 pm) and 11UTC (4.30 pm) (Fig. 5c). At this period of time, KF gives 2-mm rain and GD shows no rain, whereas as per the AWS observation, the rain was 28 mm (see Fig. 5c). All three schemes show the presence of frozen hydrometeors at  $\sim 500$  mb level at 10UTC (3.30 pm). Only BM shows the presence frozen hydrometeors at mid-level for longer duration of time (09–15UTC (2.30–8.30 pm)). The latent heat release in the formation of hydrometeor is responsible for net middle level heating rate. It may further intensify storm (Mukhopadhyay et al. 2011). Thus, the presence of more frozen hydrometeor may help the storm to intensify and enhancement of precipitation. Spatial correlation of hydrometeor occurrence, reflectivity, and rain rate from CloudSat has been reported by Marchand (2012). Thus, BM scheme could better simulate heavy rain at Pune than KF and GD, as it could produce better distribution of hydrometeor for longer time, rain water near the surface sufficiently humid, and deep layer in the lower and middle atmosphere, along with coexistence of updraft and downdrafts.

## 5 Conclusions

Weather Research and Forecasting (WRF) model experiments are carried out for pre-monsoon severe thunderstorm case of June 1, 2010 (at Pune (18.53°N, 73.85°E)). The model-simulated spatial distribution of 24-h accumulated rain (in domain 3) during the thunderstorm event shows agreement with TRMM data. Model could simulate heavy rain patch of  $>80$  mm as observed in TRMM, but all the cumulus parameterization schemes show westward shift of heavy rain patch when compared to TRMM data.

Simulated vertical structure of the temperature, RH, wind speed, and wind direction are in good agreement with the available GPS sonde profile at 08UTC (1.30 pm) (before the occurrence of storm) on 1 June at Pune. The simulated time variation in surface temperature and RH is comparable with that observed in AWS data and is less sensitive to the type of cumulus parameterization scheme. However, precipitation amounts are significantly sensitive to cumulus parameterization schemes. Stability parameters CAPE and CIN

obtained from model simulations are less than radiosonde observations at 8UTC (1.30 pm). This may be the reason that model has underestimated precipitations. Among all three schemes, the BM scheme could better simulate heavy rain at Pune. Stability parameter CAPE ( $>1,000$  J/kg) is well simulated by KF and GD that might have favored the development of storm; however, higher CIN values might have suppressed the development. In simulation with BM scheme though CAPE is moderate, CIN is also less. Hence, BM could better simulate convective storm and thus heavy rain. Model simulations with BM scheme could generate sufficiently humid and deep layer in the lower and middle atmosphere, along with the coexistence of updraft and downdraft and frozen hydrometeors at the middle level and rain water near the surface. Hence, model simulations with BM scheme could better simulate the vertical structure and time evolution of storm on June 1, 2010. The present study could examine sensitivity of the model performance to cumulus parameterization schemes. More studies are required to examine the sensitivity to planetary boundary layer (PBL) and cloud microphysics parameterization schemes in the simulation of the structure of the thunderstorm. Also, the present results are derived from the simulation of a single convective event. We propose to do simulations for large number of thunderstorms observed over Pune to generalize the results.

**Acknowledgments** Authors are thankful to Prof B. N. Goswami, Director IITM, for his constant support and encouragement. Authors also acknowledge with thanks K. K. Dani and other scientists of his group for providing the GPS sonde upper air data at Pune used in the study.

## References

- Abhilash S, Mohankumar K, Das S (2008) Simulation of microphysical structure associated with tropical cloud clusters using mesoscale model and comparison with TRMM observations. *Int J Remote Sens* 29:2411–2432
- Arakawa A (2004) The cumulus parameterization problem: past, present, and future. *J Clim* 17:2493–2525
- Asnani GC (2005) Tropical meteorology (revised edition), vol 2. Indian Institute of Tropical Meteorology, Pune
- Betts AK (1986) A new convective adjustment scheme. Part I: observational and theoretical basis. *Q J R Meteorol Soc* 112:677–692
- Betts AK, Miller MJ (1986) A new convective adjustment scheme. Part II: single column tests using GATE wave, BOMEX, ATEX, and Arctic air-mass data sets. *Q J R Meteorol Soc* 112:693–709
- Brunk IW (1949) The pressure pulsation of 11 April 1944. *J Atmos Sci* 6:181–187
- Chatterjee P, Pradhan D, De UK (2008a) Simulation of severe local storm by Mesoscale Model MM5. *Indian J Rad Space Phys* 37:419–433
- Chatterjee P, Pradhan D, De UK (2008b) Simulation of hailstorm event using Mesoscale Model MM5 with modified cloud microphysics scheme. *Ann Geophys* 26:3545–3555
- Crétat J, Pohl B, Richard Y (2011) Uncertainties in simulating regional climate of Southern Africa: sensitivity to physical parameterizations using WRF. *Clim Dyn*. doi:10.1007/s00382-011-1055-8
- Dai A (2006) Precipitation characteristics in eighteen coupled climate models. *J Clim* 19:4605–4630
- Deb SK, Kishtawal CM, Pal PK, Joshi PC (2008) Impact of TMI SST on the simulation of a heavy rainfall episode over Mumbai on 26 July 2005. *Mon Weather Rev* 136:3714–3741
- Deb SK, Kishtawal CM, Bongirwar VS, Pal PK (2010) The simulation of heavy rainfall episode over Mumbai: impact of horizontal resolutions and cumulus parameterization schemes. *Nat Hazards* 52:117–142. doi:10.1007/s11069-009-9361-8
- Deshpande M, Pattnaik S, Salvekar PS (2010) Impact of physical parameterization schemes on numerical simulation of super cyclone Gonu. *Nat Hazards* 55:211–231
- Dodla VBR, Ratna SB, Desamsetti S (2012) An assessment of cumulus parameterization schemes in the short range prediction of rainfall during the onset phase of the Indian Southwest Monsoon using MM5 Model. *Atmos Res* 120–121:249–267
- Dudhia J (1989) Numerical study of convection observed during the winter monsoon experiment using a mesoscale two dimensional model. *J Atmos Sci* 46:3077–3107

- Dudhia J (2010) WRF modeling system overview. <http://www.mmm.ucar.edu/wrf/users/tutorial/201001/WRFOverview> Dudhia.pdf
- Dudhia J, Gill D, Manning K, Wang W, Bruyere C (2003) PSU/NCAR: mesoscale modeling system tutorial class notes and user's guide: MM5 modeling system version 3. <http://www.mmm.ucar.edu/mm5/documents/tutorial-v3-notes.html>
- Gallus WA Jr (1999) Eta simulations of three extreme rainfall events: impact of resolution and choice of convective scheme. *Weather Forecast* 14:405–426
- Gemmill W, Bert K, Xu L (2007) Daily real-time global sea surface temperature—high resolution analysis at NOAA/NCEP. NOAA/NWS/NCEP/MMAB Office Note No. 260, 39
- Gilmore MS, Straka JM, Rasmussen EN (2004a) Precipitation and evolution sensitivity in simulated deep convective storms: comparisons between liquid-only and simple ice and liquid phase microphysics. *Mon Weather Rev* 132:1897–1916
- Gilmore MS, Straka JM, Rasmussen EN (2004b) Precipitation uncertainty due to variations in precipitation particle parameters within a simple microphysics scheme. *Mon Weather Rev* 132:2610–2627
- Grell GA, Dévényi D (2002) A generalized approach to parameterizing convection combining ensemble and data assimilation techniques. *Geophys Res Lett* 29:1693. doi:10.1029/2002GL015311
- He W, Ho S, Chen H, Zhou X, Hunt D, Kuo Y-H (2009) Assessment of radiosonde temperature measurements in the upper troposphere and lower stratosphere using COSMIC radio occultation data. *Geophys Res Lett* 36:L17807. doi:10.1029/2009GL038712
- Hong SY, Lim JOJ, Dudhia J (2004) The WRF single-moment 6-class microphysics scheme (WSM6). *J Korean Meteorol Soc* 42:129–151
- Hong SY, Noh Y, Dudhia J (2006) A new vertical diffusion package with an explicit treatment of entrainment processes. *Mon Weather Rev* 134:2318–2341
- Huffman GJ, Adler RF, Bolvin DT, Gu G, Nelkin EJ, Bowman KP, Hong Y, Stocker EF, Wolff DB (2007) The TRMM multisatellite precipitation analysis (TMPA): quasi-global, multiyear, combined-sensor precipitation estimates at fine scales. *J Hydrometeorol* 8. doi:10.1175/JHM560.1
- Janjic ZI (1994) The step-mountain eta coordinate model: further developments of the convection, viscous sublayer and turbulence closure schemes. *Mon Weather Rev* 122:927–945
- Janjic ZI (2000) Comments on “development and evaluation of a convection scheme for use in climate models”. *J Atmos Sci* 57:3686
- Johns RH, Doswell CA (1992) Severe local storms forecasting. *Weather Forecast* 7:588–612
- Kain JS (2004) The Kain–Fritsch convective parameterization: an update. *J Appl Meteorol* 43:170–181
- Kain JS, Fritsch JM (1993) Convective parameterization for mesoscale models: the Kain–Fritsch scheme. The representation of cumulus convection in numerical models. *Meteorol Monogr Am Meteorol Soc* 46:165–170
- Kumar A, Dudhia J, Rotunno R, Niyogi D, Mohanty UC (2008) Analysis of the 26 July 2005 heavy rain event over Mumbai, India using the Weather Research and Forecasting (WRF) model. *Q J R Meteorol Soc* 134:1897–1910
- Litta AJ, Mohankumar K (2007) Simulation of vertical structure and dynamics of thunderstorm over Cochin using MM5 mesoscale model—a case study. *Vayumandal* 1(2):51–79
- Litta AJ, Mohanty UC (2008) Simulation of a severe thunderstorm event during the field experiment of STORM programme 2006, using WRF–NMM model. *Curr Sci* 95:204–215
- Litta AJ, Chakrapani B, Mohankumar K (2007) Mesoscale simulation of an extreme rainfall event over Mumbai, India, using a high-resolution MM5 model. *Meteorol Appl* 14:291–295
- Liu C, Moncrieff MW (2007) Sensitivity of cloud-resolving simulations of warm-season convection to cloud microphysics parameterization. *Mon Weather Rev* 135:2854–2868
- Mandal M, Mohanty UC (2006) Numerical experiments for improvement in mesoscale simulation of Orissa super cyclone. *Mausam* 57:79–96
- Mandal M, Mohanty UC, Potty KVJ, Sarkar A (2003) Impact of horizontal resolution on prediction of tropical cyclones over Bay of Bengal using a regional weather prediction model. *Proc Indian Acad Sci (Earth Planet Sci)* 112:79–93
- Mandal M, Mohanty UC, Raman S (2004) A study on the impact of parameterization of the physical processes on prediction of tropical cyclones over the Bay of Bengal with NCAR/PSU mesoscale model. *Nat Hazards* 31:391–414
- Marchand R (2012) Spatial correlation of hydrometeor occurrence, reflectivity, and rain rate from CloudSat. *J Geophys Res* 117:D06202. doi:10.1029/2011JD016678
- McCumber M, Tao WK, Simpson J (1991) Comparison of ice-phase microphysical parameterization schemes using numerical simulation of tropical convection. *J Appl Meteorol* 30:985–1004



- Melissa AG, Mullen SL (2005) Evaluation of QPF from a WRF ensemble system during the southwest monsoon. Presented at the 6th WRF/15th MM5 users' workshop, June 27–30, National Center for Atmospheric Research
- Mlawer EJ, Taubman SJ, Brown PD, Iacono MJ, Clough SA (1997) Radiative transfer for inhomogeneous atmosphere: RRTM, a validated correlated-k model for the long wave. *J Geophys Res* 102: 16663–16682
- Mohan M, Bhati S (2011) Analysis of WRF model performance over subtropical region of Delhi, India. *Adv Meteorol*. doi:10.1155/2011/621235
- Molinari J, Romps DM, Vollaro D, Nguyen L (2012) CAPE in tropical cyclones. *J Atmos Sci* 69:2452–2463
- Mukhopadhyay P, Sanjay J, Cotton WR, Singh SS (2005) Impact of surface meteorological observations on RAMS forecast of monsoon weather systems over the Indian region. *Meteorol Atmos Phys* 90:77–108
- Mukhopadhyay P, Taraphdar S, Goswami BN (2011) Influence of moist processes on track and intensity forecast of cyclones over the north Indian Ocean. *Geophys Res* 116:D05116. doi:10.1029/2010JD014700
- Osuri KK, Mohanty UC, Routray A, Kulkarni MA, Mohapatra M (2012) Customization of WRF-ARW model with physical parameterization schemes for the simulation of tropical cyclones over North Indian Ocean. *Nat Hazards* 63:1337–1359
- Patra KP, Santhanam MS, Potty KVI, Tewari M, Rao PLS (2000) Simulation of tropical cyclones using regional weather prediction models. *Curr Sci* 79:70–78
- Rajeevan M, Kesarkar A, Thampi SB, Rao TN, Radhakrishna B, Rajasekhar M (2010) Sensitivity of WRF cloud microphysics to simulations of a severe thunderstorm event over Southeast India. *Ann Geophys* 28:603–619
- Rama Rao YV, Hatwar HR, Salah AK, Sudhakar Y (2007) An experiment using the high resolution Eta and WRF models to forecast heavy precipitation over India. *Pure appl Geophys* 164:1593–1615
- Ramalingeswara Rao S, Krishna KM, Bhanu Kumar OSRU (2009) Study of tropical cyclone “Fanoos” using MM5 model—a case study. *Nat Hazards Earth Syst Sci* 9:43–51
- Rao DVB, Prasad DH (2006) Numerical prediction of Orissa super cyclone (1999): sensitivity to the parameterization of convection, boundary layer and explicit moisture processes. *Mausam* 57:61–78
- Rao DVB, Prasad DH (2007) Sensitivity of tropical cyclone intensification to boundary layer and convective processes. *Nat Hazards* 41:429–445
- Reisner J, Rasmussen RJ, Bruintjes RT (1998) Explicit forecasting of super cooled liquid water in winter storms using the MM5 mesoscale model. *Q J R Meteorol Soc* 124B:1071
- Romps DM, Kuang Z (2010) Do undiluted convective plumes exist in the upper tropical troposphere? *J Atmos Sci* 67:468–484
- Skamarock WC (2004) Evaluating mesoscale NWP models using kinetic energy spectra. *Mon Weather Rev* 132:3019–3032
- Srinivas CV, Venkatesan R, Rao DVB, Prasad DH (2007) Numerical simulation of Andhra Severe Cyclone (2003): model sensitivity to the boundary layer and convection parameterization. *Pure appl Geophys* 164:1465–1487
- Sukrit K, Somporn C, Jiemjai K (2010) Mesoscale simulation of a very heavy rainfall event over Mumbai, using the Weather Research and Forecasting (WRF) model. *Chiang Mai J Sci* 37(3):429–442
- Trivedi DK, Mukhopadhyay P, Vaidya SS (2006) Impact of physical parameterization schemes on the numerical simulation of Orissa super cyclone. *Mausam* 57:97–110
- Turtiainen H, Jauhianinen H, Lentonen J, Survo P, Viitanen VP, Dabberdt WF (2010) Upper atmosphere humidity measurements with the APS sensor—1st progress Report on the Vaisala Reference Radiosonde Program. In: 15th symposium on meteorological observation and instrumentation, Atlanta, GA, 17–21 Jan 2010
- Vaidya SS, Kulkarni JR (2007) Simulation of heavy precipitation over Santacruz, Mumbai on 26 July 2005, using mesoscale model. *Meteorol Atmos Phys* 98:55–66